Hierarchical feature extraction on functional brain networks for autism spectrum disorder identification with resting-state fMRI data

Yiqian Luo^a, Qiurong Chen^a, Fali Li^b, Liang Yi^{c,d}, Peng Xu^{a,b,*} and Yangsong Zhang^{a,b,*}

ARTICLE INFO

Keywords:
Autism spectrum disorder
fMRI
Functional connectivity network
Graph convolution
Functional gradients

ABSTRACT

Autism spectrum disorder (ASD) is a pervasive developmental disorder of the central nervous system, which occurs most frequently in childhood and is characterized by unusual and repetitive ritualistic behaviors. Currently, diagnostic methods primarily rely on questionnaire surveys and behavioral observation, which may lead to misdiagnoses due to the subjective evaluation and measurement used in these traditional methods. With the advancement in medical imaging, MR imaging-based diagnosis has become an alternative and more objective approach. In this paper, we propose a Hybrid neural Network model for ASD identification, termded ASD-HNet, to hierarchically extract features on the functional brain networks based on resting-state functional magnetic resonance imaging data. This hierarchical method can better extract brain representations, improve the diagnostic accuracy, and help us better locate brain regions related to ASD. Specifically, features are extracted from three scales: local regions of interest (ROIs) scale, community-clustering scale, and the whole-communities scale. For the ROI scale, graph convolution is used to transfer features between ROIs. At the community cluster scale, functional gradients are introduced, the clustering algorithm K-Means is used to automatically cluster ROIs with similar functional gradients into several communities, and features of ROIs belonging to the same community are extracted to characterize these communities. At global information integration scale, we extract global features from community-scale brain networks to characterize the whole brain networks. We validate the effectiveness of our method using the public dataset of Autism Brain Imaging Data Exchange I (ABIDE I), and elucidate the interpretability of the method. Experimental results demonstrate that the proposed ASD-HNet can yield superior performance than compared methods.

1. Introduction

Autism spectrum disorder (ASD) is a type of pervasive developmental disorder affecting the central nervous system (Pandolfi et al., 2018), approximately 1% of the world's population is affected by ASD. Moreover, ASD is associated with a high incidence of concurrent disorders, such as depression and anxiety (Vohra et al., 2017). Autism generally occurs in childhood, and its impairment may remain lifelong, and parts of individuals with ASD require lifelong support (Lord et al., 2018). ASD encompasses a range of symptoms, such as social communication disorders and restrictive repetitive behaviors (Hirota and King, 2023; Bhat et al., 2014). Autism is extremely damaging to the physical and mental health of patients, and significantly affects the lives of affected individuals and their families. However, due to the lack of specific pathogenesis, it is very challenging to make an accurate diagnosis.

Unfortunately, there are no definitive drugs and methods for the treatment of ASD, and the pathological mechanisms of ASD remain for further exploring (Geschwind, 2009). Currently, the most effective approach is to provide

ORCID(s):

advanced behavioral training for individuals with ASD, implement early intervention for ASD, and correct the problem behaviors of autistic patients. This necessitates the early and accurate diagnosis of individuals with ASD, which is crucial. However, by the time the individual exhibits the corresponding behaviors, the patient may miss the optimal treatment time, which makes treatment more difficult. At present, most diagnostic methods are still through questionnaires and behavioral observation to determine whether an individual has ASD (American Psychiatric Association et al., 2013). This method has strong subjectivity and is influenced by the environment, which can lead to a higher risk of misdiagnosis (Wang et al., 2022). There is an urgent need for a highly accurate pathological diagnostic method and the identification of more autism-related biomarkers to aid in diagnosis.

Benefiting from the rapid development of medical image technology, imaging-based approaches provides us with important tools to analyze and study neurophysiology. Functional magnetic resonance imaging (fMRI), as a non-invasive neuroimaging technique (Matthews and Jezzard, 2004), can measure the blood oxygen level dependent (BOLD) changes caused by neuronal activity throughout the brain at a series of time points (Friston et al., 1994). Many studies have demonstrated the feasibility of using resting state functional magnetic resonance imaging (rs-fMRI) to

^aLaboratory for Brain Science and Artificial Intelligence, School of Computer Science and Technology, Southwest University of Science and Technology, Mianyang, China

^bMOE Key Laboratory for NeuroInformation, Clinical Hospital of Chengdu Brain Science Institute, and Center for Information in BioMedicine, School of Life Science and Technology, University of Electronic Science and Technology of China, Chengdu, China

^cDepartment of Neurology, Sichuan Provincial People's Hospital, University of Electronic Science and Technology of China, Chengdu, China

^dChinese Academy of Sciences Sichuan Translational Medicine Research Hospital, Chengdu, China

^{*}Corresponding author

reveal interactions between regions of interest (ROIs) in the brain of people with mental illness (Dvornek et al., 2018). In recent years, numerous researchers have integrated deep learning technology with rs-fMRI to conduct corresponding exploration and research on mental diseases, yielding significant achievements (Dong et al., 2020; Luppi et al., 2022). Most studies divide the brain into multiple ROIs using prefabricated brain templates, obtain the BOLD time series of ROIs, and then calculate the BOLD time series correlation between ROIs to obtain the brain functional connectivity network (FCN) for corresponding analysis and exploration of the brain (Dong and Sun, 2024; Wang et al., 2023; Hong et al., 2019).

The brain FCN extracted from resting-state fMRI data can reflect the functional interactions between brain regions, which serves as a very effective representation tool to explore the normal and altered brain function (Van Den Heuvel and Pol, 2010). At present, numerous deep learning methods utilize brain FCNs to implement ASD identification. For instance, Eslami et al. proposed using a data-driven linear approach to enhance the training data and using autoencoders to achieve the diagnosis of ASD (Eslami et al., 2019). Kawahara et al. proposed a network architecture called Brain-NetCNN, which has special edge-to-edge, edge-to-node, and node-to-graph convolutional filters, and takes into account the non-Euclidean nature of brain networks (Kawahara et al., 2017). Jiang et al. proposed a graph network model Hi-GCN, which first extracts the features of each subject using the ROI-level graph network, and then constructs a population graph network with the extracted features of each subject as nodes (Jiang et al., 2020). Hi-GCN takes into account the spatial properties of brain networks, as well as the structure of the network directly between people. Recently, the DGAIB model proposed by Dong et al. (Dong and Sun, 2024) has utilized graph neural networks to carry out effective feature transmission in brain regions, combining an information bottleneck to filter out irrelevant information related to the target task, thereby applying the retained effective features to improve classification performance. Dong et al. proposed to build an individualized and a common functional connectivity networks, and then use the proposed multiview brain Transformer module to carry out parallel feature extraction learning for the two FCNs (Dong et al., 2024). Finally, the characteristics of the two branches are fused to make the final diagnosis classification.

In recent years, there has been some progress in the research of constructing multi-scale brain network to realize the diagnosis and classification of ASD. For instance, Liu et al. used a set of atlases for multiscale brain parcellation, and then progressively extracted functional connectivity networks from small scale to large scale by constructing mapping relationships between different scale brain maps (Liu et al., 2023a). Similarly, Bannadabhavi et al. proposed a community-aware approach by using two different scales of altas and then constructing a map of ROIs to communities based on the division of the two brain atlas (Bannadabhavi et al., 2023). Then transformer (Vaswani et al., 2017)

is used to extract ROI-scale network into community-scale brain network for corresponding diagnosis and classification. However, the existing methods all need to manually divide the mapping relationship between ROIs and communities, which is very complicated and cumbersome.

Previous deep learning models often lack the exploration and application of physiological mechanisms, as well as multi-scale features mining, e.g. from local regions to global brain scale, resulting in suboptimal diagnostic performance of the models. In current study, we combine rs-fMRI with deep learning techniques to design a network model from a brain physiology perspective, aiming to boost the detection performance on ASD. We propose a hybrid neural network model for ASD identification, termded ASD-HNet, to hierarchically extract features on the functional brain networks at three scales, i.e., local ROI scale, communityclustering scale, and whole-communities scale. Specifically, we use the AAL template (Tzourio-Mazoyer et al., 2002) to divide the brain into 116 ROIs, extract the BOLD signals in each ROI, and then calculate the functional connectivity network. Then, the graph convolutional network (GCN) (Niepert et al., 2016) is used to transfer information between ROIs. After that, we use functional gradients to automatically cluster ROIs into several communities instead of using another scale of prefabricated atlas. In this way, ROIs with similar functions are clustered into a community, allowing us to obtain the community-scale features. Finally, we perform global brain convolution on the community-scale features to integrate features on global scale. Furthermore, based on the features obtained by the ASD-HNet, we introduced prototype learning for classification to achieve better identification results. The experiments on the public dataset of Autism Brain Imaging Data Exchange I (ABIDE I) verified the superior performance of the proposed ASD-HNet.

2. Materials and Methodology

2.1. Functional Gradients

The functional gradients of the brain can provide a more comprehensive perspective by capturing the continuous spatial patterns of connectivity outside the segregated networks in the human brain (Guell et al., 2018; Huntenburg et al., 2018). A gradient-based approach, which is a nonlinear decomposition of high-dimensional rest-state functional connectivity (rs-FC), can identify brain functional levels by representing brain connectivity in a continuous, low-dimensional space (Dong et al., 2020). Functional gradients have been widely applied in brain analysis (Dong et al., 2020; Guo et al., 2023; Gong and Zuo, 2023). In the analysis of various mental diseases, functional gradients can obviously reflect the abnormal functional hierarchy of brain regions.

The functional gradients were also used to study the ASD. For instance, Hong et al. (Hong et al., 2019) found functional gradients disorder in autistic patients, which showed that the functional distances between the transmodal regions and the unimodal regions decreased, that is, the functional independence of the brain region was reduced.

 Table 1

 Demographic information of subjects from ABIDE-I dataset.

Dataset	Category	Subject	Gender(M/F)	$Age(Mean \pm std)$
ABIDE	ASD	396	347/49	17.78 ± 9.01
	HC	452	371/81	16.75 ± 7.25

Urchs et al. used ABIDE-I dataset (Di Martino et al., 2014) to carry out corresponding functional gradients analysis for autism, and also revealed the compression of gradients (less functional separation) in ASD (Urchs et al., 2022). Although functional gradients has been used in data analysis for ASD, combining functional gradients with deep learning for classification and diagnosis of ASD remain to be explored. In this paper, we proposed a deep learning model by leveraging functional gradients to achieve better ASD identification performance.

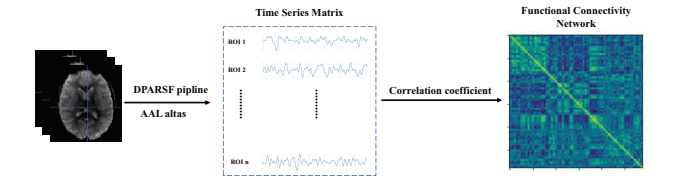


Figure 1: The pipelines process and computation of functional connectivity network.

2.2. Materials and data preprocessing

To verify the performance of the proposed method, we conducted the experiment on the publicly available ABIDE-I dataset, including rs-fMRI and phenotypic data of 1112 subjects from 17 different sites (Di Martino et al., 2014; Craddock et al., 2013). In current study, we utilized rs-fMRI data from 848 subjects, including 396 patients with ASD and 452 health controls (HCs). The demographic information of the studied subjects is reported in Table 1.

For data preprocessing, we used the data Processing Assistant for Resting-State fMRI (DPARSF) to preprocess rsfMRI data (Yan and Zang, 2010). The specific steps are as follows: (1) Discarding the first 5 volumes. (2) Correcting of slice-related delay. (3) Correcting head movement. (4) Using EPI template normalization in MNI space, resampling to 3 mm resolution of $3 \times 3 \times 3$. (5) Smoothing with a 4 mm full-width at half-maximum (FWHM) Gaussian kernel. (6) Linear detrending and temporal band-pass filtering of BOLD signal (0.01-0.10 Hz). (7) Harmful signals that return head movement parameters, white matter, cerebrospinal fluid (CSF), and global signals. The registered fMRI volumes are then partitioned into 116 ROIs using the AAL template, and BOLD time series are obtained for each ROI. Based on these time series of all the ROIs, we obtained the brain FCN matrix by calculating the Pearson correlation coefficient with the formula (1).

$$\rho_{ij} = \frac{\sum_{t=1}^{T} \left(i_t - \overline{i} \right) \left(j_t - \overline{j} \right)}{\sqrt{\sum_{t=1}^{T} \left(i_t - \overline{i} \right)^2} \sqrt{\sum_{t=1}^{T} \left(j_t - \overline{j} \right)^2}}$$
(1)

Here i_t and j_t ($t = 1, 2, \dots, T$) represent the time series of i-th and j-th brain regions, and the \bar{i} and \bar{j} are the average of two time series of brain region i and j, respectively. T represents the total length of time series.

2.3. Proposed Method

The schematic diagram of the proposed ASD-HNet is shown in Figure 2. This model is designed to progressively extract the discriminative and robust representations based on FCNs from three different scales, i.e., local ROI scale, community-clustering scale, and whole-communities scale, to achieve ASD identification. More details are described below.

2.3.1. The local ROI scale

The suspicious connections calculated with the formula (1) could exist in the FCN, and they can degrade the classification performance of the model using raw FCN as input. To eliminate the influence, we adopted the *F*-score (Chen and Lin, 2006) as a global feature selector to screen the features in the FCN. For each subject, since their FCN is a real symmetric matrix, we utilized the upper or lower triangle elements of the FCN matrix as the screened features which are then unfolded to a vector. Subsequently, we computed the *F*-score for each element in the vector by the formula (2).

$$F_{i} = \frac{\left(\overline{x_{i}^{ASD}} - \overline{x_{i}}\right)^{2} + \left(\overline{x_{i}^{HC}} - \overline{x_{i}}\right)^{2}}{\frac{1}{N_{ASD} - 1} \sum_{k=1}^{N_{ASD}} \left(x_{k,i}^{ASD} - \overline{x_{i}^{ASD}}\right)^{2} + \frac{1}{N_{HC} - 1} \sum_{k=1}^{N_{HC}} \left(x_{k,i}^{HC} - \overline{x_{i}^{HC}}\right)^{2}}$$
(2)

where $\overline{x_i}$, $\overline{x_i^{ASD}}$, $\overline{x_i^{HC}}$ represent the grand average of the i-th feature of all subjects, the group average of i-th feature of ASD subjects and the i-th feature of HC subjects, respectively. N_{ASD} and N_{HC} denote the number of ASD subjects and HC subjects. The $x_{k,i}^{ASD}$ and $x_{k,i}^{HC}$ refers to the i-th feature of the k-th ASD subject and k-th HC subject, respectively.

With the *F*-score, we can obtain two sparse FCN matrices. We kept 10% of the connections in the functional connectivity matrix to create a sparse FCN matrix, which was used to create a graph network. Besides, we removing half of connections in the functional connectivity matrix to create another sparse FCN matrix, which was used as the node features in the graph network.

Based on these two sparse FCN matrices, we constructed a ROI-scale graph network G(V, E), where V is the node eigenmatrix and E is the adjacency matrix. Then, we used

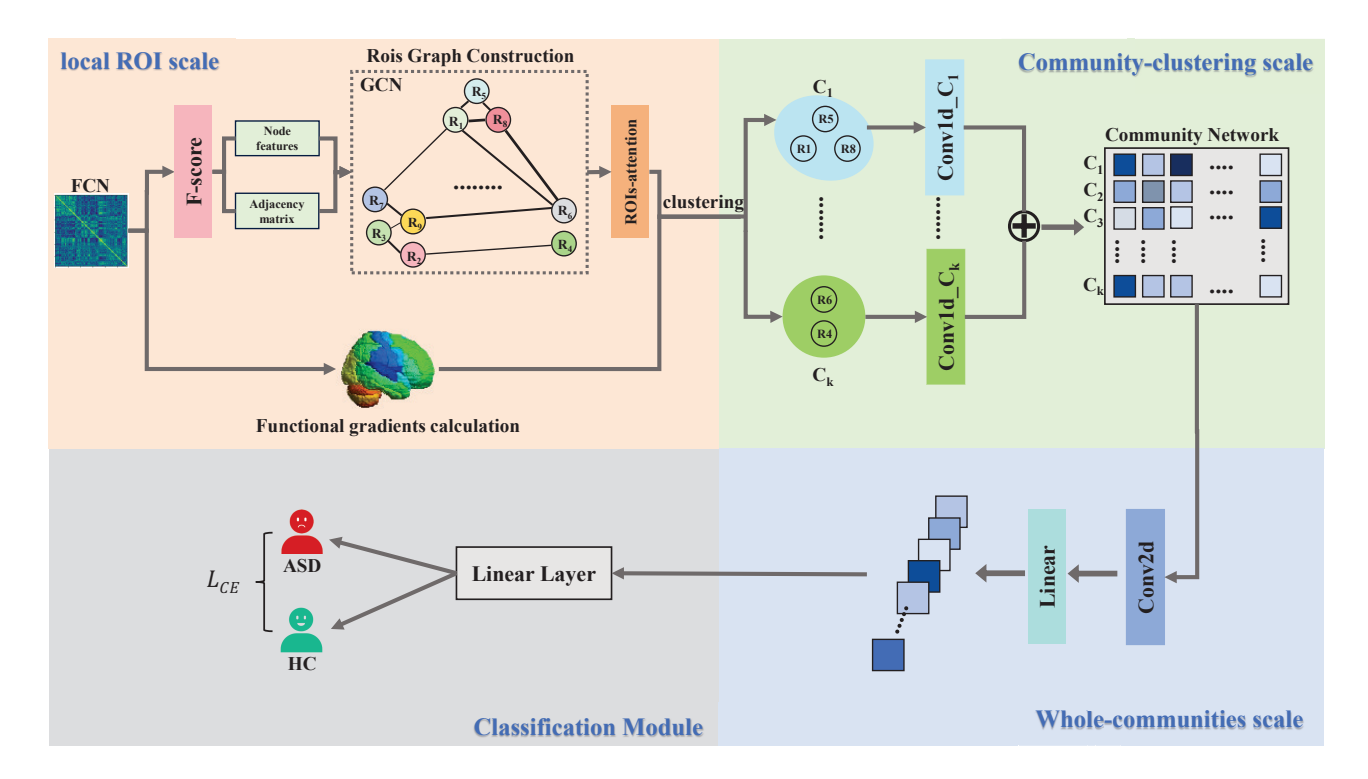


Figure 2: The diagram of the proposed hybrid neural network model for ASD identification (ASD-HNet).

graph convolutional neural network to conduct feature extraction on the ROI-level scale. Here, we used one layer of spatial-based GCN to complete the message transfer between ROIs, the specific implementation is as follows:

$$H = \sigma (E \cdot V \cdot W) \tag{3}$$

where W is a layer-specific trainable weight matrix with the shape (116, 64) and σ is the activation function. In order to make nodes pay attention to their own characteristics, the diagonal elements of the adjacency matrix E are all set to 1.

After graph convolution, we further employed a ROI-level attention mechanism to weight each ROI features. Sepcifically, we initialized an attention weight H_{atten} with all values set to 1, and then used two successive fully connected layers to learn the attention weight for each ROI. The operation of one fully connected layer is shown in the following formula (4). It should be noted that since ROIs are weighted using positive numbers, so the activation function (σ_{atten}) was ReLU in the fully connected layer.

$$H_{atten}^{\dagger} = \sigma_{atten} \left(W_{atten}^{\dagger} H_{atten} + Bias_{atten}^{\dagger} \right) \tag{4}$$

After obtaining the attention weights of ROIs, we used these weights to multiple each ROI, and then used a residual connection to fuse the weighted and original ROI-level features, following by a batch normalization operation, as shown in formula (5).

$$H^{\dagger} = BN \left(H_{atten}^{\dagger} \odot H + H \right) \tag{5}$$

where BN denotes the BatchNorm1d operation and \odot represents the dot product operation.

2.3.2. The community-clustering scale

The brain's community network comprises groups of functionally similar ROIs, each with a high degree of functional concentration. Community networks are crucial for understanding the functional organization of the brain (Van Den Heuvel et al., 2009). Functional communities have been shown to be relevant to understanding cognitive behavior (Van Den Heuvel and Pol, 2010), mental states (Geerligs et al., 2015), and neurological and psychiatric disorders (Canario et al., 2021). We used second module further extracted functional features at community-clustering scale as shown in Figure 2. Since functional gradients can well reflect the functional similarity between ROIs, we proposed to use functional gradients to automatically cluster ROIs into community networks.

We utilized whole group-level (include ASD subjects and HC subjects) average functional connectivity matrix inputs into BrainSpace (Vos de Wael et al., 2020) to obtain group-level functional gradients. In general, the calculation of functional gradients is mainly divided into two steps. The first step is to sparse the input matrix (the sparsity is 10%), and then select a kernel function to calculate the affinity matrix. In the second step, the functional gradients are obtained

by using nonlinear dimensionality reduction on the resulting affinity matrix. In our work, we chose cosine similarity as kernel function to calculate the affinity matrix (A(i,j)). The calculation formula is as follows:

$$A(i,j) = \cos sim\left(R_i, R_j\right) = \frac{R_i R_j^{Tr}}{\left\|R_i\right\| \left\|R_j\right\|}$$
 (6)

where R_i and R_j represent the feature vectors of the *i*-th and *j*-th ROI in the FCN, respectively. And $\|\cdot\|$ denotes the l_2 -norm, Tr stands for transpose operation.

For nonlinear dimensionality reduction, we employed the diffusion mapping technique in current study. We calculated the diffusion matrix using the previously obtained affinity matrix A(i, j). The specific calculation process is as follows.

$$P_{\beta} = D_{\beta}^{-1} W_{\beta} \tag{7}$$

where W_{β} is defined as formula (8), D_{β} is the degree matrix derived from W_{β} .

$$W_{\beta} = D^{-1/\beta} A D^{-1/\beta} \tag{8}$$

where A is the affinity matrix, and D is the degree matrix of A. β is the anisotropic diffusion parameter used by the diffusion operator, whose value is empirically set to 0.5 (Vos de Wael et al., 2020). Finally, the functional gradients of multiple components were obtained by calculating the eigenvalues and eigenmatrices of P_{β} .

The first N_{gra} components of the functional gradients of each ROI were taken as input, and the unsupervised algorithm K-means was used to complete the clustering of ROIs. In this way, 116 ROIs were clustered into k communities according to functional similarity. Then we customized a one-dimensional convolution for each community to extract the ROIs features in this community as a representation of this community. The features extraction of each community can be summarized in the following formula.

$$C_{i} = \sigma \left(LN \left(conv1D_{i} \left(ROIs_{i} \right) \right) \right) \tag{9}$$

where $ROIs_i$, LN, and σ represent the feature matrix of ROIs belonging to the *i*-th community, layernorm, and activation function, respectively. And $conv1D_i$ is a one-dimensional convolution operation specific to each community. The parameter settings of the $conv1D_i$ are listed in Table 2.

2.3.3. The whole-communities scale and classification

By extracting community-clustering scale features, we obtained a community-level network with the shape (k, 64). In order to further extract high-level features, Conv2D was used to extract global integration information on whole-communities scale. The parameter settings of Conv2D are listed in Table 2.

In order to train the model serving as feature extractor, after the whole-communities scale module, we used a liner

layer and a softmax layer to achieve the supervised classification task. After the model was trained, we used it as feature extractor (denoted as $f(\cdot)$), the outputs of the whole-communities scale module were used as the features.

To implement the classification, the prototype learning was used, which achieves classification by learning a set of prototypes, representing the centers of different classes (Qiu et al., 2024). Prototype learning using extracted multiperspective brain representations:

$$P_{i} = \frac{1}{K} \sum_{k} f\left(FC_{k,i}\right) \tag{10}$$

where $P_i(i = 1, 2)$ is the prototype of class i, K represents the number of samples in each class, and $FC_{k,i}$ corresponds to the FCN of the k-th subject in the i-th class.

For the final classification of test subjects, we calculated the Euclidean distance between the feature vectors of the test samples and the two prototypes. Each test sample was then assigned to the category of the prototype with minimal distance, as shown in Figure 3.

2.4. Compared methods

To demonstrate the performance of our proposed method, we compared ASD-HNet with state-of-the art methods, which are listed as follows.

2.4.1. f-GCN

F-GCN is a basic graph convolutional network. The focus of this method is to choose the appropriate threshold to remove redundant connections, with the optimal threshold identified in our experiment being 0.1. In f-GCN, multiple GCN layers are stacked. The model employs a global average pooling operator to generate a coarse graph, which reduces the number of parameters by decreasing the size of the representation and thus helps avoid overfitting. The readout layer then consolidates the node representations into a single graph representation (Jiang et al., 2020).

2.4.2. BrainnetCNN

Kawahara et al. proposed a new convolutional model named BrainnetCNN. BrainNetCNN incorporates specific convolutional and pooling layer designs to capture the complex relationships and features within brain networks. Typically, BrainNetCNN includes the following three main components, i.e., Edge-to-Edge (E2E) layer, Edge-to-Node (E2N) layer, Node-to-Graph (N2G) layer (Kawahara et al., 2017). By combining these layers, BrainNetCNN effectively extracts useful features from brain network data.

2.4.3. CNN-model

Sherkatghanad et al. proposed a two-dimensional convolution of multiple different kernels to extract features at different levels, including features of single ROI and correlation features between ROIs (Sherkatghanad et al., 2020). And then the classification is achieved by fusing the features of different levels. In the end, the convolution with four different kernels performed best on processed data. For simplicity, we termed it as CNN-model, hereafter.

 Table 2

 Detailed architecture and parameters of community-clustering scale and whole-communities scale.

Block	Layer	Output size	Explanation		
	Input	$(N_i, 64)$	N _i stands for the number of ROIs belonging to community i		
Conv1d		(1, 64)	outchannel=1,kernel_size=15,padding='same',stride=1		
Conv1D _i LayerNorm $(1, 64)$					
Activation (1, 64)		(1, 64)			
	Dropout (1, 64)		dropout rate=0.3		
	Concatenate	(k, 64)	The features of k communities are concatenated to form a community network		
	unsqueeze	(1, k, 64)			
Conv2D Conv2d (16, 1, 1)		(16, 1, 1)	outchannel=16,kernelsize=(k, 64),stride=1		
	squeeze	(16)			
Linear	Linear	(16)	in features=16,out features=16		
Lilical	Activation	(16)	At this point, we have obtained a feature representation of the whole brain		

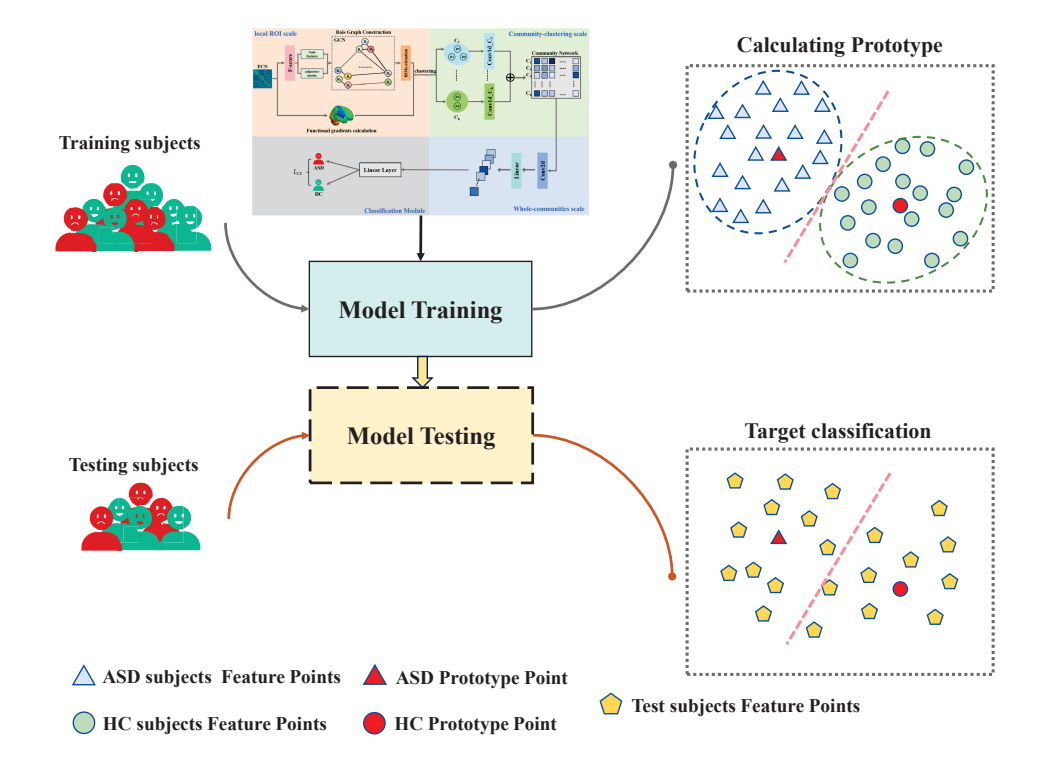


Figure 3: Workflow of prototype learning based classification. First, we use the training set to train the feature extractor, then calculate the corresponding prototype for each category. Finally, we obtain the features of the test data using the trained feature extractor and calculate the distance to each prototype for final classification result.

2.4.4. FBNETGEN

FBNETGEN is a learnable method to construct the adjacency matrix and explores the interpretability of the generated brain network for downstream tasks. Specifically, the method uses 1D-CNN and bi-GRU as encoders to learn the features of the time series, and then obtains the learned adjacency matrix by multiplying the learned features with its own transpose. Finally, graph convolution is used to implement the final classification task (Kan et al., 2022a).

2.4.5. ASD-DiagNet

ASD-DiagNet is a collaborative learning strategy that combines single-layer perceptron and autoencoder. For the

input data, a linear data enhancement approach is used to augment the training data for better feature extraction (Eslami et al., 2019).

2.4.6. BrainTransformerNet

BrainTransformerNet leverages transformer to learn the edge attention of functional connectivity and extract an interpretable functional network. In this approach, a new readout function is also designed to take advantage of modular level similarities between ROIs in the brain network for better brain representation (Kan et al., 2022b).

 Table 3

 Hyper-parameters setting for the proposed model.

	Hyperparameter	Setting
1	Optimezer	Adam
2	Learning rate	0.0001
3	Dropout rate	0.3
4	Training batch size	32
5	Activation function	$Tanh(\cdot)$
6	Loss	CrossEntropy

2.4.7. Hi-GCN

Hi-GCN takes the features of each subject extracted by f-GCN as nodes, and gets the edges between subjects through the calculation of correlation coefficients. After that, the population graph networks is bulit. Then, four-layer residual graph convolution is used to achieve feature transfer between subjects, and the learned feature representation of each subject is obtained to realize the final classification task (Jiang et al., 2020).

2.4.8. MCG-Net

Luo et al. proposed a dual-branch network architecture, MCG-Net. This method employs parallel convolution and graph convolution to respectively extract high-order representations and low-order spatial features of functional connectivity networks. Ultimately, the extracted multi-features are fused and utilized in a downstream classification task through linear layers. (Luo et al., 2023).

2.5. Experimental setting and evaluation metrics

In our experiment, we employed the 10-fold cross-validation strategy to conduct the comparison among different models. The data were divided into 10 folds, with 9 folds used for training and 1 fold used for testing. The models were implemented with PyTorch framwork, and all the experiments were conducted on a GeForce RTX 3090 GPU.

We adopted the adaptive moment estimation optimizer (Adam) to train the model with using cross-entropy as the loss function. More hyperparameter settings in the model are listed in Table 3. The cross entropy loss function is defined as below:

$$L_{CE} = \frac{1}{N} \sum_{i}^{N} -[y_i \times \log(p_i) + (1 - y_i) \times \log(1 - p_i)]$$

$$\tag{11}$$

where N denotes the number of training subjects, y_i is the true label of the i-th subject, and p_i stands the predicted probability.

For the hyperparameters N_{gra} and k, we set them to be 2 and 7 during the experiments, respectively, because Gong et al. found the first two gradients account for most of the variance of the functional connectivity network (Gong and Zuo, 2023), and Yeo et al. found network template communities (Yeo et al., 2011). In subsection 3.3, we will disscuss the influence of different settings on the classification performance.

In order to evaluate the model, four metrics, i.e., sensitivity (Sen), specificity (Spe), accuracy (Acc), and F1, were applied as evaluation indicators. The final values of these metrics were averaged across ten results from 10-fold cross-validation. The definitions were as follows:

$$Acc = \frac{TP + TN}{TP + FN + FP + TN} \tag{12}$$

$$Sen = \frac{TP}{TP + FN} \tag{13}$$

$$Spe = \frac{TN}{TN + FP} \tag{14}$$

$$F1 = \frac{2TP}{2TP + FP + FN} \tag{15}$$

where TP, FN, TN and FP represent the number of ASD subjects correctly classified, the number of ASD subjects wrongly classified as HC subjects, the number of HC subjects correctly classified, the number of HC subjects wrongly classified as ASD subjects, respectively.

3. Results and discussion

3.1. Performance comparison among different methods

The classification results of the ASD-HNet and compared methods are shown in Table 4, with the same experimental settings. All the results of the compared methods were obtained by reproducing the models according to the public codes provided in the references. The hyperparameters were set according to the original studies, except for f-GCN and Hi-GCN. During training the f-GCN and Hi-GCN, we set the corresponding optimal threshold to be 0.1 and 0.2 respectively. It can be found that the proposed ASD-HNet outperforms other methods on all four indicators, with accuracy improved by 3.09%, sensitivity improved by 2.94%, specificity improved by 1.38% and F1-score improved by 2.45%, respectively.

To further evaluate the performance of ASD-HNet, we also compared our ASD-HNet method to other four methods that performed well on the ABIDE dataset, i.e., MC-NFE (Wang et al., 2022), MVS-GCN (Wen et al., 2022), MBT (Dong et al., 2024) and DGAIB (Dong and Sun, 2024). In these studies, the authors adopted different amounts of data and different brain templates. Namely, MC-NFE used a total of 609 subjects recruited from 21 sites in ABIDE-I and ABIDE-II (Wang et al., 2022). The MVS-GCN used 871 subjects from 17 different sites, including 403 patients with ASD and 468 normal subjects (Wen et al., 2022). MBT chose 1035 subjects, including 505 patients diagnosed with ASD and 530 healthy controls (Dong et al., 2024). DGAIB pooled 1096 subjects from 17 sites in ABIDE-I, consisting

Table 4Performance comparison of among the proposed models and other models. The best results are marked in bold. The results marked with an asterisk (*) are reproduced .

Method	Accuracy(%)	Sensitivity(%)	Specificity(%)	F1-score(%)
f-GCN*	61.32	61.28	61.31	59.13
BrainnetCNN*	64.52	59.84	68.46	61.03
CNN-model*	64.88	58.55	69.70	60.36
FBNETGEN*	67.14	69.69	64.65	68.59
ASD-DiagNet*	66.70	60.64	71.91	62.56
BrainTransformerNet*	67.00	64.23	70.23	67.14
Hi-GCN*	67.34	68.78	65.70	65.17
MCG-Net*	70.48	67.08	73.52	68.32
ASD-HNet	73.57	72.63	74.90	71.04

Table 5Comparison with state-of-the-art methods(ABIDE), with best results shown in bold. '-' indicates the experiment results are not reported on the dataset.

Method	MC-NFE	MVS-GCN	MBT	DGAIB	ASD-HNet
(ASD/HC)	(Wang et al., 2022)	(Wen et al., 2022)	(Dong et al., 2024)	(Dong and Sun, 2024)	(Ours)
(ASD/TIC)	(280/329)	(403/468)	(505/530)	(527/569)	(396/452)
Altas	BASC-064	AAL-116	AAL-116	AAL-90	AAL-116
ACC(%)	68.42	68.92	72.08	71.20	73.57
SEN(%)	70.05	69.09	72.26	69.60	72.63
SPE(%)	63.64	63.15	71.50	73.41	74.90
F1-score(%)	-	-	71.69	71.39	71.04

of 569 healthy controls and 527 individuals diagnosed with ASD (Dong and Sun, 2024).

For a intuitive comparison between these method and our ASD-HNet, we directly quoted the reported results from originial references as some previous studies (Wang et al., 2022). In these studies, the authors did not release the implementation codes, or did not describe how to generate the used data from ABIDE dataset. The comparison results are summarized in Table 5. By this rough comparison, we can also find that although the F1-score of our method is little lower than MBT and DGAIB methods, our method achieved the best accuracy (73.57%), sensitivity (72.63%) and specificity (74.90%).

3.2. Ablation experiment

To analyze the rationality and effectiveness of the architecture of the proposed model, we conducted several ablation experiments to check whether removing each key module will degrade the overall performance. Accordingly, in order to verify that the ROI-scale graph convolution has effective information transfer and whether the ROI-attention module is effective in improving the model performance, we conducted a comparative test with/without GCN and ROI-attention. Similarly, we only used the orignal linear layer during training the feature extractor to achieve the classification to test the validity of prototype learning. The results of the ablation experiment were shown in Table 6.

Through the ablation experiment results, we can find that the performance of the model decreased significantly after the elimination of three modules respectively. Although removing prototype learning decreased the specificity, the proposed model could provide higher sensitivity for effectively diagnosing the ASD subjects, and achieved more balanced performance on the two metrics of sensitivity and specificity.

3.3. The influence of the hyperparameters settings on the model performance

In ASD-HNet, two hyperparameters N_{gra} and k need to be configured, which represent the number of functional gradients components and the number of categories for clustering, respectively. The results reported above were obtained when N_{gra} and k were set to be 2 and 7. Different combination of these two hyperparameters may yield different classification performance. Therefore, we carried out experiments to check the influence of the hyperparameters settings on the model performance, with k ranged from 5 to 10 and N_{gra} ranged from 2 to 6. The experimental results are shown in Figure 4. The highest score for each indicator is marked with a red circle.

From the results in the Figure 4, we can find that although the best combination of hyperparameter values in the sensitivity index is different from the other three indicators, the three indicators of accuracy, specificity and F1-score all achieve the best scores when k=7 and $N_{gra}=2$. Moreover, sensitivity has the third highest score under this combination of hyperparameter values. Based on comprehensive evaluation, setting the k=7 and N_{gra} as 7 and 2 was a viable choice. Besides, these settings matched the findings in previous studies, such as the first two gradients can account for most of the variance of the functional connectivity network (Gong and Zuo, 2023), and there exists Yeo 7 network template communities (Yeo et al., 2011).

Table 6
The results of ablation experiments. The best results are marked in bold.

Method	Accuracy(%)	Sensitivity(%)	Specificity(%)	F1-score(%)
w\o ROI-scale GCN	70.12	67.58	72.51	68.13
w\o ROI-attention	71.79	69.85	73.53	70.04
w\o Prototype Leanrning	72.86	67.83	77.07	69.82
ASD-HNet	73.57	72.63	74.90	71.04

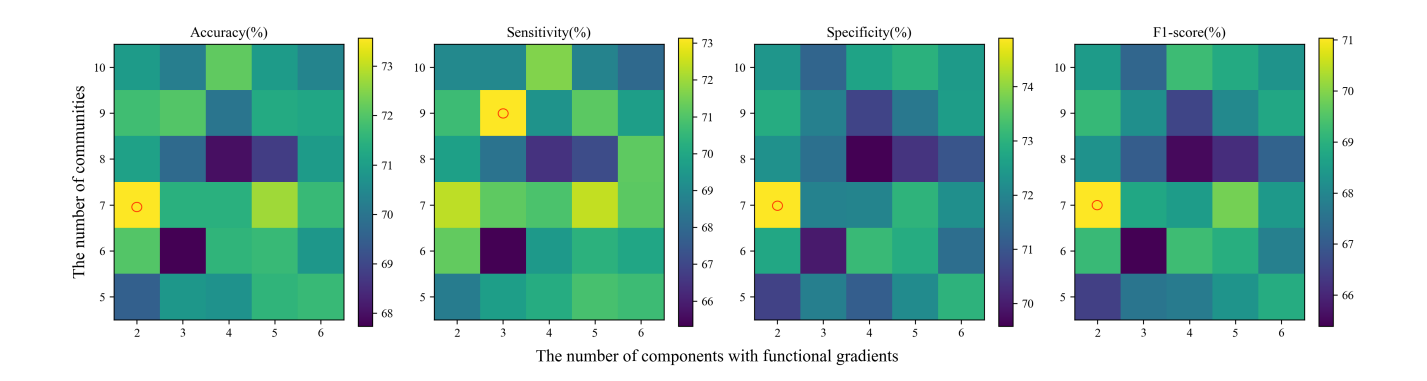


Figure 4: The averaged four metrics obtained by different combination of k and N_{gra} .

3.4. The interpretability and visualization analysis

In this section, we investigate whether the proposed model can find the discriminative features that can be explained with previous neural mechanisms.

First, we want to check whether the model can find the difference patterns of FCN between ASD subjects and HCs subjects. F-score is a technique for extracting key features based on a data-driven approach. For the analysis of key edges of brain regions, we retained the 50% edges with the highest F-score for retention and visualization, as shown in Figure 5. All the visualization are achieved with Brain-Net Viewer (Xia et al., 2013) tool. The most differentiated edges observed in Figure 5 are mostly the connections between the temporal lobe, the frontal lobe and the sensorimotor area, which is consistent with previous findings. For instance, Abrams et al. has reported an atypical decline in functional connectivity between the temporal area (auditory network) and the medial prefrontal area (DMN) in people with autism (Abrams et al., 2013).

Furthermore, we want to show that the functional gradients in the model can find the difference patterns on the community networks. We conducted the analysis of the validity and interpretability of utilizing the first two components of functional gradients for constructing community networks. Since the gradients calculated separately for the two groups of levels may not be directly comparable (Vos de Wael et al., 2020), we chose the joint embedding (Xu et al., 2020) to realize the alignment of the two groups of functional gradients. Then we conducted individual analyses of both the principal and secondary gradients, as well as a joint analysis of the

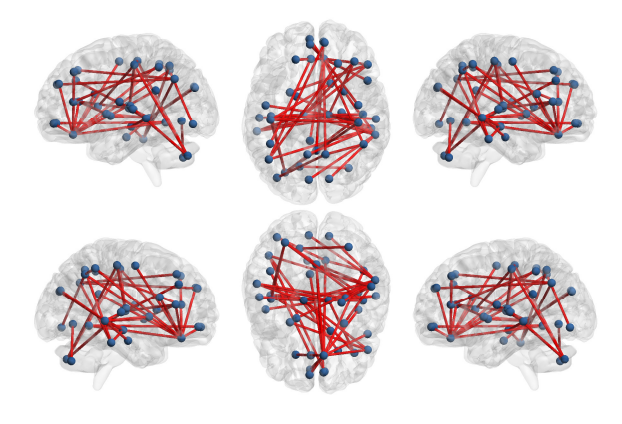


Figure 5: The edges of the brain regions with the greatest difference between HC and ASD patients.

principal and secondary gradients.

The aligned functional gradients of the ASD and HC groups are used to find the ten ROIs with the largest difference in absolute values of the principal gradients of the two groups. The same method is used to find the ten ROIs with the biggest difference in the secondary gradient between the two groups. The brain regions with the greatest differences in the principal gradients are found to be right parahippocampal gyrus (PHG.R), left superior frontal gyrus of orbital part (ORBsup.L), right supe-

rior parietal gyrus (SPG.R), right cerebellum inferior (CR-BLCrus2.R), left middle occipital gyrus (MOG.L), left middle frontal gyrus (MFG.L), vermis (Vermis45), right precuneus (PCUN.R), right paracentral lobule (PCL.R), right hippocampus (HIP.R). The result is shown in the Figure 6.

The ten ROIs with the largest difference in the secondary gradient are right Supplementary motor area (SMA.R), left Precental gyrus (PreCG.L), left Posterior cingulate gyrus (PCG.L), right Inferior parietal, but supramarginal and angular gyri (IPL.R), left Middle occipital gyrus (MOG.L), Vermis (Vermis45), right Inferior frontal gyrus of orbital part (ORBinf.R), left Middle temporal gyrus (MTG.L), right Precuneus (PCUN.R), right Middle temporal gyrus (MTG.R). The result is shown in the Figure 7.

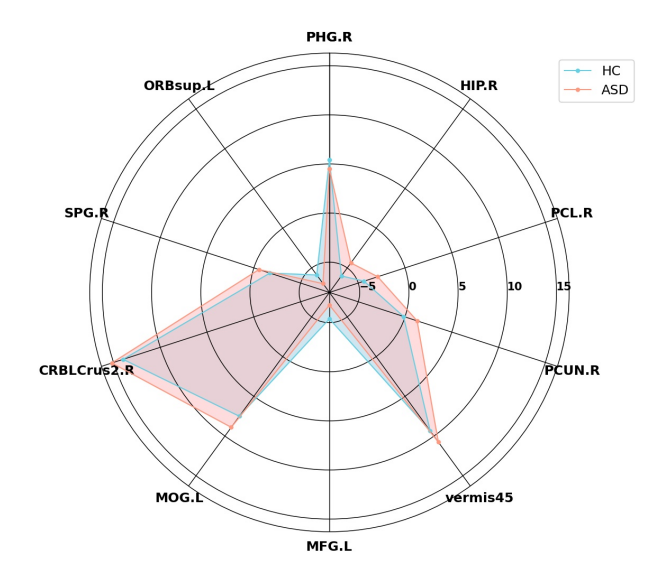


Figure 6: The ten ROIs with the largest difference in group principal gradients.

Right after that, we merged the first two gradients (principal and secondary gradients) and employed Euclidean distance (consistent with K-Means algorithm) to measure the distinction in corresponding ROIs between the ASD and HC groups. Subsequently, we visualized the ten brain regions with the greatest Euclidean distance (indicating the most significant difference). The visualized result is shown in Figure 8.

Based on the aforementioned findings, disparities in the attention towards specific brain regions are observed between the principal and secondary gradients. For instance, the principal gradient demonstrated a higher focus on the left frontal lobe, whereas the secondary gradient prioritizes the left temporal lobe. By concurrently considering the first two gradients, a more comprehensive evaluation of functional differences and similarities among brain regions can be attained, consequently leading to an improved community clustering effect. Our conclusion suggested that the

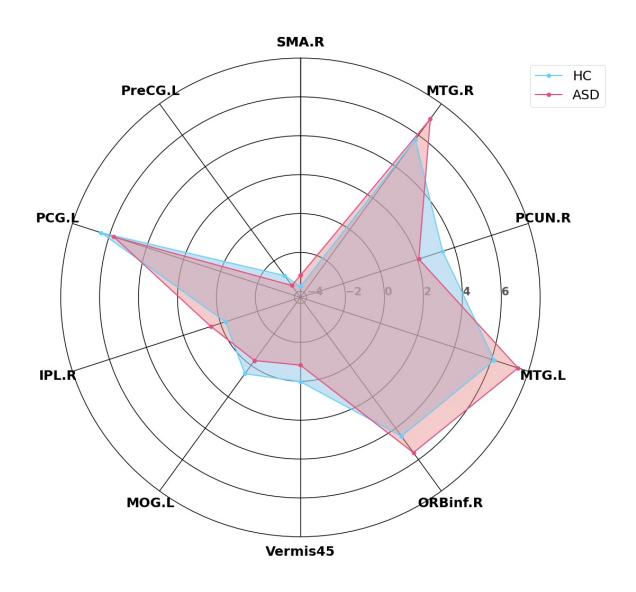


Figure 7: The ten ROIs with the largest difference in the secondary gradients.

variations in brain regions among ASD patients primarily manifest in the superior frontal gyrus of the orbital part, precuneus, and several regions within the temporal lobe. This is similar to (Hong et al., 2019) in discovery roughly.

3.5. Experiments on model generalization

In order to investigate the generalization of our proposed method, as some previous studies (Zhang et al., 2023; Liu et al., 2023b), we used the proposed model to conduct classification on a ADHD-200 Consortium (ADHD-200) dataset ¹. We choose the dataset preprocessed by Athena pipeline (Bellec et al., 2017). A total of 759 subjects from 7 sites were contained for fMRI data, including 303 ADHD patients and 456 HCs. Similar to the above experiments on ASD, we used 10-fold cross-validation to conduct corresponding experiments. Initially, for ASD-HNet, we used the same hyperparameters as we did for classifying ASD. We then tuned the model based on the specifics of the ADHD data. The adjustments were as follows: (1) Due to the imbalance in the ADHD data, we used a larger batchsize (64) to ensure that each batch included a more balanced representation of both classes. (2) Given the presence of multiple subtypes of ADHD (Molavi et al., 2020), we incorporated more global brain features from different perspectives to enhance the model's discriminative ability. Specifically, we increased the out_channels of conv2d in the global brain scale to 32. These adjustments can enhance the model's adaptation and optimization for classifying ADHD.

In addition to the comparative methods mentioned above for ASD, we also included two state-of-the-art methods in our analysis: (1) MDCN (Yang et al., 2023), which utilize

¹http://fcon_1000.projects.nitrc.org/indi/adhd200/

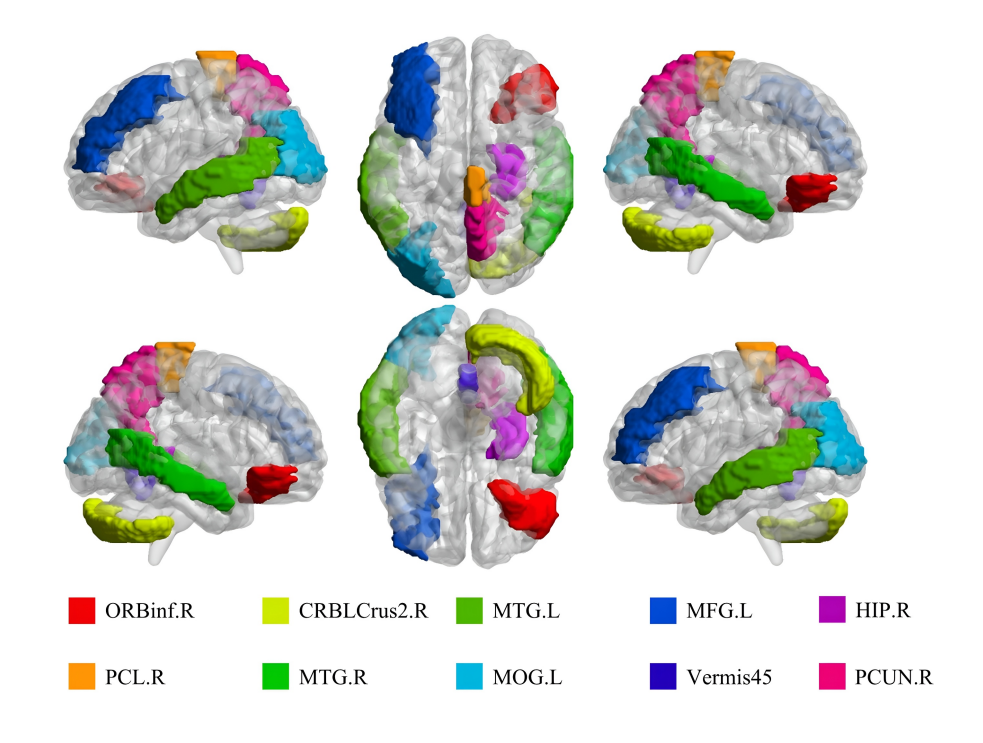


Figure 8: The ten ROIs with the greatest differences in the first two gradients.

fMRI data from 572 subjects, including 261 ADHD patients and 311 healthy controls (HCs); (2) A-GCL (Zhang et al., 2023), which uses data from 947 subjects, comprising 362 ADHD patients and 585 HCs. The experimental results are shown in Table 7. The results indicate that our method also achieves better performance in classifying ADHD. Due to the imbalance in the data we used, the comparison methods we reproduced show a significant imbalance in specificity and sensitivity, resulting in a lower F1-score. However, our method achieves the best performance in terms of accuracy (71.33%) and specificity (80.30%). This demonstrated that ASD-HNet not only performs well in classifying ASD but also achieved good classification performance for ADHD, which validates its robustness and generalization.

3.6. Limitation

Even though ASD-HNet achieved better performance than other methods, some limitations still exist in this study. First of all, the classification performance is still unsatisfactory and can not be applied to clinical scenes in current stage. External cohort dataset should be collected for further validation (Han et al., 2019; Wang et al., 2021). The proposed method relies on a large amount of data for corresponding training. When the amount of data is insufficient or unbalanced, how to maintain the performance of the model is an important issue worthy of further research. Besides, we did not consider the large variability among the dataset from different sites into the model construction. It is beneficial to explicitly eliminate the differences on data distribution with

some technologies, such as domain adaption (Wang et al., 2019; Wen et al., 2024; Liu et al., 2023c). In future, we need address these issues during designing models to conduct the multi-site fMRI data analysis.

4. Conclusion

In this work, we proposed a hybrid neural network model to hierarchically extract features on the functional brain networks for ASD identification. Extensive experiments demonstrate the effectiveness of the proposed model. Compared with other baseline methods, the proposed model achieve superior performance on widely used dataset ABIDE-I. The ablation experiments and the interpretability analysis further verify the rationality of the model architecture. The generalization performance was also explored preliminarily on the ADHD-200 dataset. In future studies, it is benifical to integrate neural mechanisms into the deep learning models to boost the ASD identification.

CRediT authorship contribution statement

Yiqian Luo: Methodology, Software, Validation, Writing-Original Draft, Writing-Review and Editing, Visualization. Qiurong Chen: Software, Writing-Review and Editing. Fali Li: Methodology, Writing-Review and Editing. Liang Yi: Writing-Review and Editing. Peng Xu: Conceptualization, Methodology, Writing-Review and Editing. Yangsong Zhang: Supervision, Conceptualization, Methodology, Writing-Review and Editing.

Table 7Experimental results of ASD-HNet on ADHD-200 data, with best results shown in bold. '*' stands that the method has not been reproduced, and the results shown are those reported in the original study and '-' indicates the experiment results are not reported on the dataset. "Tuned" denotes the adjustments made to ASD-HNet through fine-tuning.

ADHD-200	Method	ACC(%)	SEN(%)	SPE(%)	F1-score(%)
	f-GCN	61.12	83.47	27.43	30.95
	BrainnetCNN	62.53	49.64	71.84	51.01
	CNN-based	64.13	43.69	77.64	49.33
	Hi-GCN	66.01	78.96	46.58	51.82
	MCG-Net	68.67	53.30	79.41	57.26
(ADHD/HC)	MDCN* (261/311)	67.45	71.97	62.39	66.86
	A-GCL* (362/585)	70.92	-	-	-
Ours	ASD-HNet	70.00	57.22	78.53	60.44
	ASD-HNet (tuned)	71.33	58.49	80.30	61.80

References

- Abrams, D.A., Lynch, C.J., Cheng, K.M., Phillips, J., Supekar, K., Ryali, S., Uddin, L.Q., Menon, V., 2013. Underconnectivity between voice-selective cortex and reward circuitry in children with autism. Proceedings of the National Academy of Sciences 110, 12060–12065.
- American Psychiatric Association, D., Association, A.P., et al., 2013. Diagnostic and statistical manual of mental disorders: DSM-5. American psychiatric association Washington, DC.
- Bannadabhavi, A., Lee, S., Deng, W., Ying, R., Li, X., 2023. Community-aware transformer for autism prediction in fmri connectome, in: International Conference on Medical Image Computing and Computer-Assisted Intervention, Springer. pp. 287–297.
- Bellec, P., Chu, C., Chouinard-Decorte, F., Benhajali, Y., Margulies, D.S., Craddock, R.C., 2017. The neuro bureau adhd-200 preprocessed repository. NeuroImage 144, 275–286.
- Bhat, S., Acharya, U.R., Adeli, H., Bairy, G.M., Adeli, A., 2014. Automated diagnosis of autism: in search of a mathematical marker. Reviews in the Neurosciences 25, 851–861.
- Canario, E., Chen, D., Biswal, B., 2021. A review of resting-state fmri and its use to examine psychiatric disorders. Psychoradiology 1, 42–53.
- Chen, Y.W., Lin, C.J., 2006. Combining svms with various feature selection strategies. Feature extraction: foundations and applications, 315–324.
- Craddock, C., Benhajali, Y., Chu, C., Chouinard, F., Evans, A., Jakab, A., Khundrakpam, B.S., Lewis, J.D., Li, Q., Milham, M., et al., 2013. The neuro bureau preprocessing initiative: open sharing of preprocessed neuroimaging data and derivatives. Frontiers in Neuroinformatics 7, 5.
- Di Martino, A., Yan, C.G., Li, Q., Denio, E., Castellanos, F.X., Alaerts, K., Anderson, J.S., Assaf, M., Bookheimer, S.Y., Dapretto, M., et al., 2014. The autism brain imaging data exchange: towards a large-scale evaluation of the intrinsic brain architecture in autism. Molecular psychiatry 19, 659–667.
- Dong, C., Sun, D., 2024. Brain network classification based on dynamic graph attention information bottleneck. Computer Methods and Programs in Biomedicine 243, 107913.
- Dong, D., Luo, C., Guell, X., Wang, Y., He, H., Duan, M., Eickhoff, S.B., Yao, D., 2020. Compression of cerebellar functional gradients in schizophrenia. Schizophrenia bulletin 46, 1282–1295.
- Dong, Q., Cai, H., Li, Z., Liu, J., Hu, B., 2024. A multiview brain network transformer fusing individualized information for autism spectrum disorder diagnosis. IEEE Journal of Biomedical and Health Informatics , 1–12.
- Dvornek, N.C., Ventola, P., Duncan, J.S., 2018. Combining phenotypic and resting-state fmri data for autism classification with recurrent neural networks, in: 2018 IEEE 15th International Symposium on Biomedical Imaging (ISBI 2018), IEEE. pp. 725–728.
- Eslami, T., Mirjalili, V., Fong, A., Laird, A.R., Saeed, F., 2019. Asd-

- diagnet: a hybrid learning approach for detection of autism spectrum disorder using fmri data. Frontiers in neuroinformatics 13, 70.
- Friston, K.J., Jezzard, P., Turner, R., 1994. Analysis of functional mri timeseries. Human brain mapping 1, 153–171.
- Geerligs, L., Rubinov, M., Henson, R.N., et al., 2015. State and trait components of functional connectivity: individual differences vary with mental state. Journal of Neuroscience 35, 13949–13961.
- Geschwind, D.H., 2009. Advances in autism. Annual review of medicine 60, 367–380.
- Gong, Z.Q., Zuo, X.N., 2023. Connectivity gradients in spontaneous brain activity at multiple frequency bands. Cerebral Cortex 33, 9718–9728.
- Guell, X., Schmahmann, J.D., Gabrieli, J.D., Ghosh, S.S., 2018. Functional gradients of the cerebellum. elife 7, e36652.
- Guo, S., Feng, L., Ding, R., Long, S., Yang, H., Gong, X., Lu, J., Yao, D., 2023. Functional gradients in prefrontal regions and somatomotor networks reflect the effect of music training experience on cognitive aging. Cerebral Cortex 33, 7506–7517.
- Han, S., Wang, Y., Liao, W., Duan, X., Guo, J., Yu, Y., Ye, L., Li, J., Chen, X., Chen, H., 2019. The distinguishing intrinsic brain circuitry in treatment-naïve first-episode schizophrenia: Ensemble learning classification. Neurocomputing 365, 44–53.
- Hirota, T., King, B.H., 2023. Autism spectrum disorder: A review. Jama 329, 157–168.
- Hong, S.J., Vos de Wael, R., Bethlehem, R.A., Lariviere, S., Paquola, C., Valk, S.L., Milham, M.P., Di Martino, A., Margulies, D.S., Smallwood, J., et al., 2019. Atypical functional connectome hierarchy in autism. Nature communications 10, 1022.
- Huntenburg, J.M., Bazin, P.L., Margulies, D.S., 2018. Large-scale gradients in human cortical organization. Trends in cognitive sciences 22, 21–31.
- Jiang, H., Cao, P., Xu, M., Yang, J., Zaiane, O., 2020. Hi-gcn: A hierarchical graph convolution network for graph embedding learning of brain network and brain disorders prediction. Computers in Biology and Medicine 127, 104096.
- Kan, X., Cui, H., Lukemire, J., Guo, Y., Yang, C., 2022a. Fbnetgen: Task-aware gnn-based fmri analysis via functional brain network generation, in: International Conference on Medical Imaging with Deep Learning, PMLR, pp. 618–637.
- Kan, X., Dai, W., Cui, H., Zhang, Z., Guo, Y., Yang, C., 2022b. Brain network transformer. Advances in Neural Information Processing Systems 35, 25586–25599.
- Kawahara, J., Brown, C.J., Miller, S.P., Booth, B.G., Chau, V., Grunau, R.E., Zwicker, J.G., Hamarneh, G., 2017. Brainnetcnn: Convolutional neural networks for brain networks; towards predicting neurodevelopment. NeuroImage 146, 1038–1049.
- Liu, M., Zhang, H., Shi, F., Shen, D., 2023a. Hierarchical graph convolutional network built by multiscale atlases for brain disorder diagnosis

- using functional connectivity. IEEE Transactions on Neural Networks and Learning Systems , 1-13.
- Liu, R., Huang, Z.A., Hu, Y., Zhu, Z., Wong, K.C., Tan, K.C., 2023b. Spatial-temporal co-attention learning for diagnosis of mental disorders from resting-state fmri data. IEEE Transactions on Neural Networks and Learning Systems, 1–15.
- Liu, X., Wu, J., Li, W., Liu, Q., Tian, L., Huang, H., 2023c. Domain adaptation via low rank and class discriminative representation for autism spectrum disorder identification: A multi-site fMRI study. IEEE Transactions on Neural Systems and Rehabilitation Engineering 31, 806–817.
- Lord, C., Elsabbagh, M., Baird, G., Veenstra-Vanderweele, J., 2018. Autism spectrum disorder. The lancet 392, 508–520.
- Luo, Y., Li, N., Pan, Y., Qiu, W., Xiong, L., Zhang, Y., 2023. Aided diagnosis of autism spectrum disorder based on a mixed neural network model, in: International Conference on Neural Information Processing, Springer, pp. 150–161.
- Luppi, A.I., Mediano, P.A., Rosas, F.E., Holland, N., Fryer, T.D., O'Brien, J.T., Rowe, J.B., Menon, D.K., Bor, D., Stamatakis, E.A., 2022. A synergistic core for human brain evolution and cognition. Nature Neuroscience 25, 771–782.
- Matthews, P.M., Jezzard, P., 2004. Functional magnetic resonance imaging. Journal of Neurology, Neurosurgery & Psychiatry 75, 6–12.
- Molavi, P., Nadermohammadi, M., Salvat Ghojehbeiglou, H., Vicario, C.M., Nitsche, M.A., Salehinejad, M.A., 2020. Adhd subtype-specific cognitive correlates and association with self-esteem: A quantitative difference. BMC psychiatry 20, 1–10.
- Niepert, M., Ahmed, M., Kutzkov, K., 2016. Learning convolutional neural networks for graphs, in: International conference on machine learning, PMLR. pp. 2014–2023.
- Pandolfi, V., Magyar, C.I., Dill, C.A., 2018. Screening for autism spectrum disorder in children with down syndrome: An evaluation of the pervasive developmental disorder in mental retardation scale. Journal of Intellectual & Developmental Disability 43, 61–72.
- Qiu, L., Li, J., Zhong, L., Feng, W., Zhou, C., Pan, J., 2024. A novel eeg-based parkinson's disease detection model using multiscale convolutional prototype networks. IEEE Transactions on Instrumentation and Measurement 73, 1–14.
- Sherkatghanad, Z., Akhondzadeh, M., Salari, S., Zomorodi-Moghadam, M., Abdar, M., Acharya, U.R., Khosrowabadi, R., Salari, V., 2020. Automated detection of autism spectrum disorder using a convolutional neural network. Frontiers in neuroscience 13, 482737.
- Tzourio-Mazoyer, N., Landeau, B., Papathanassiou, D., Crivello, F., Etard, O., Delcroix, N., Mazoyer, B., Joliot, M., 2002. Automated anatomical labeling of activations in spm using a macroscopic anatomical parcellation of the mni mri single-subject brain. Neuroimage 15, 273–289.
- Urchs, S.G., Tam, A., Orban, P., Moreau, C., Benhajali, Y., Nguyen, H.D., Evans, A.C., Bellec, P., 2022. Functional connectivity subtypes associate robustly with asd diagnosis. Elife 11, e56257.
- Van Den Heuvel, M.P., Mandl, R.C., Kahn, R.S., Hulshoff Pol, H.E., 2009. Functionally linked resting-state networks reflect the underlying structural connectivity architecture of the human brain. Human brain mapping 30, 3127–3141.
- Van Den Heuvel, M.P., Pol, H.E.H., 2010. Exploring the brain network:

- a review on resting-state fmri functional connectivity. European neuropsychopharmacology 20, 519–534.
- Vaswani, A., Shazeer, N., Parmar, N., Uszkoreit, J., Jones, L., Gomez, A.N., Kaiser, L., Polosukhin, I., 2017. Attention is all you need, in: Advances in neural information processing systems, pp. 6000–6010.
- Vohra, R., Madhavan, S., Sambamoorthi, U., 2017. Comorbidity prevalence, healthcare utilization, and expenditures of medicaid enrolled adults with autism spectrum disorders. Autism 21, 995–1009.
- Vos de Wael, R., Benkarim, O., Paquola, C., Lariviere, S., Royer, J., Tavakol, S., Xu, T., Hong, S.J., Langs, G., Valk, S., et al., 2020. Brainspace: a toolbox for the analysis of macroscale gradients in neuroimaging and connectomics datasets. Communications biology 3, 103.
- Wang, J., Wang, X., Wang, R., Duan, X., Chen, H., He, C., Zhai, J., Wu, L., Chen, H., 2021. Atypical resting-state functional connectivity of intra/inter-sensory networks is related to symptom severity in young boys with autism spectrum disorder. Frontiers in Physiology 12.
- Wang, M., Zhang, D., Huang, J., Yap, P.T., Shen, D., Liu, M., 2019. Identifying autism spectrum disorder with multi-site fMRI via low-rank domain adaptation. IEEE Transactions on Medical Imaging 39, 644–655.
- Wang, N., Yao, D., Ma, L., Liu, M., 2022. Multi-site clustering and nested feature extraction for identifying autism spectrum disorder with restingstate fmri. Medical image analysis 75, 102279.
- Wang, Y., Genon, S., Dong, D., Zhou, F., Li, C., Yu, D., Yuan, K., He, Q., Qiu, J., Feng, T., et al., 2023. Covariance patterns between sleep health domains and distributed intrinsic functional connectivity. Nature Communications 14, 7133.
- Wen, G., Cao, P., Bao, H., Yang, W., Zheng, T., Zaiane, O., 2022. Mvs-gcn: A prior brain structure learning-guided multi-view graph convolution network for autism spectrum disorder diagnosis. Computers in biology and medicine 142, 105239.
- Wen, L., Chen, S., Xie, M., Liu, C., Zheng, L., 2024. Training multisource domain adaptation network by mutual information estimation and minimization. Neural Networks 171, 353–361.
- Xia, M., Wang, J., He, Y., 2013. Brainnet viewer: a network visualization tool for human brain connectomics. PloS one 8, e68910.
- Xu, T., Nenning, K.H., Schwartz, E., Hong, S.J., Vogelstein, J.T., Goulas, A., Fair, D.A., Schroeder, C.E., Margulies, D.S., Smallwood, J., et al., 2020. Cross-species functional alignment reveals evolutionary hierarchy within the connectome. Neuroimage 223, 117346.
- Yan, C., Zang, Y., 2010. Dparsf: a matlab toolbox for "pipeline" data analysis of resting-state fmri. Frontiers in systems neuroscience 4, 1377.
- Yang, Y., Ye, C., Ma, T., 2023. A deep connectome learning network using graph convolution for connectome-disease association study. Neural Networks 164, 91–104.
- Yeo, B.T., Krienen, F.M., Sepulcre, J., Sabuncu, M.R., Lashkari, D., Hollinshead, M., Roffman, J.L., Smoller, J.W., Zöllei, L., Polimeni, J.R., others., 2011. The organization of the human cerebral cortex estimated by intrinsic functional connectivity. Journal of Neurophysiology 106, 1125–1165.
- Zhang, S., Chen, X., Shen, X., Ren, B., Yu, Z., Yang, H., Jiang, X., Shen, D., Zhou, Y., Zhang, X.Y., 2023. A-gcl: Adversarial graph contrastive learning for fmri analysis to diagnose neurodevelopmental disorders. Medical Image Analysis 90, 102932.